Proceedings of the 5th International Conference on Civil Engineering Fundamentals and Applications (ICCEFA 2024)
Lisbon, Portugal- November 18 - 20, 2024
Paper No.134
DOI: 10.11159/iccefa24.134

Inhibition of Karstification Progressing In Soluble Rocks under Water Pressure Using Chemical Grouts

Aram Aziz[1, 2], Mehrdad Ghahremani[1], Seyed Mohammad Fattahi[1], Abbas Soroush[1], Seyed Mohammad Reza Imam[1]
[1] Amirkabir University of Technology
Hafez Avenue-1591634311, Tehran, Iran
aramaziz@aut.ac.ir; m.gh11@aut.ac.ir; fattahi.m.s@aut.ac.ir; soroush@aut.ac.ir; rimam@aut.ac.ir
[2] Koya University
Erbil, KRI, Iraq

Abstract **-** Karstification is considered a common geologic phenomenon in soluble rocks (gypsum/anhydrite) that poses a vast challenge to engineering structures, especially hydraulic structures, due to water seepage with high pressure and velocity under this type of structure. Hence, improving the soluble rocks in the presence of water is imperative. In this study, the dissolution behavior of gypsum rock and the improvement of its solubility have been investigated. To perform this, karstification (gypsum rock dissolution) was simulated by creating a hole in the center of the gypsum samples and subjecting them to hydraulic shear stress under different head pressures. Additionally, to control the karstification of soluble rocks two commercially available liquid polymers, polyurethane (PU) and a mixture of acrylic and cement (ARC) were used to treat the soluble rocks. The rock samples extracted from Fatha Formation outcrop at vicinity of Mosul Dam site. Two sets of experiments were conducted on untreated and chemical grout-treated samples. The obtained findings reveal that the solubility of gypsum increases with the increase in water pressure, and (PU) and (ARC) are the influential chemical grouts in halting the solubility of the gypsum rock samples during the experimental duration.

Keywords**:** dissolution, gypsum/anhydrite, karstification, chemical improvement, Mosul Dam, and water pressure.

1. Introduction

Soluble rocks such as gypsum and rock salt dissolve in the presence of water. Therefore, In areas such as gypsum mines and dams located on gypsum rock, when the gypsum is exposed to water, the dissolution and erosion of the gypsum may cause severe damage to the infrastructure and cause irreparable financial and human losses [1, 2]. Therefore, investigating the solubility behavior and improving the solubility characteristics of soluble rocks is essential.

Grouts may be categorized as the traditional (i.e., cement, fly ash, lime, bitumen, etc.) and non-traditional (e.g., polyurethane, acrylate, sodium silicate) [3]. The main advantages of the polymer grouts are their high penetrability, low viscosity, controllability of the gelling time and high adhesivity. These characteristics make them viable alternatives to traditional cement [4, 5].

PU is categorized as a polymer that results from the combination of polyol (-OH) and isocyanate (-NCO). Depending on its reaction with water, PU is classified into hydrophobic and hydrophilic. Hydrophobic absorb minimal additional water. In contrast, hydrophilic grouts have assimilate significant amounts of water into their chemical structure. PU is frequently employed in civil engineering for sealing cracks and soil improvement [6].

Acrylic polymers or thin film coatings represent another category of polymers. In recent years, there has been an increasing adoption of thin film coatings within the engineering field, particularly for applications like soil and rock stabilization [1]. The popularity of thin film coatings in engineering referred to their wide range of properties, like flexibility and excellent adhesion, mechanical strength, scratch resistance, and thermal stability [8, 9]. The effect of liquid acrylic polymer on the geotechnical properties of fine-grained soils shows that the used slurry does not have a significant effect on Atterberg limits and unconfined compressive strength; nonetheless, it did influence CBR results [5]

Numerous efforts have been made to improve gypseous soils, with a specific emphasis on enhancing their mechanical properties [10-13]. Surprisingly, published research regarding the chemical treatments to control the gypsum solubility is scarce. Considering this gap, the primary objective of this research is to study the efficacy of two commercial liquid polymers, including polyurethane (PU) and acrylic-cement mixture (ARC) to control the solubility of gypsum. In this study, treated and untreated samples were used to check the solubility of gypsum.

2. Materials and Methods

2.1. Gypsum rocks and Sampling

This study utilizes gypsum samples measuring 50 mm x 90 mm, which are categorized into two groups: untreated and treated . In untreated samples, a 6 mm diameter hole is drilled in the center, while treated samples undergo the creation of an 8 mm diameter hole initially, followed by reduction to 6 mm diameter using polyurethane and acrylic polymer liquid. (Fig.1)

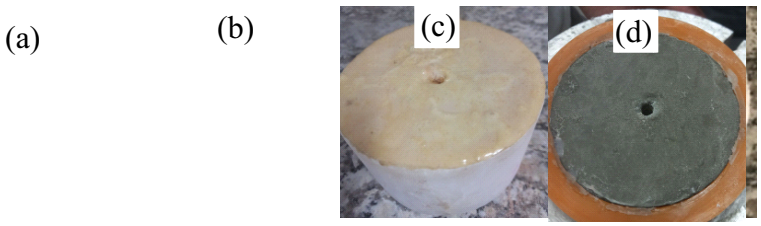

Fig. 1: Gypsum rock samples; a) untreated before test; b) untreated after test; d) PU treated; d) ARC treated

Table.1 displays the X-ray Fluorescence (XRF) outcomes, while Fig.2 depicts the X-ray diffraction (XRD) findings of the samples. The XRF findings indicate the presence of oxides of primary elements such as Ca, S, and LOI, which constitute gypsum. Furthermore, the XRD outcomes confirm gypsum as the primary crystal constituent, affirming the use of pure gypsum in this study.

Table 1: XRF results of gypsum samples.

Sample Name	SiO_2	Al_2O_3	Fe_2O_3	CaO	MgO	Na_2O	K_2O	TiO_2	MnO	SO_3	LOI *
dissolution	-	-	-	32.48	-	0.096	-	0.019	0.006	45.4	20.88

LOI= loss on ignition.

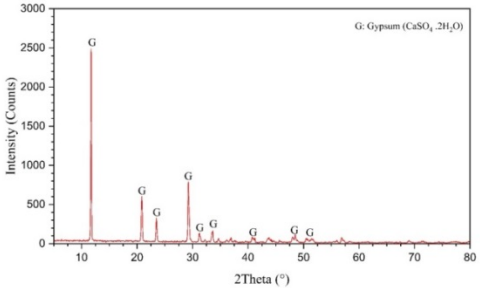

Fig.2. XRD analysis of gypsum samples.

2.2 Acrylic polymer liquid

In this study, the emulsion liquid acrylic polymer was combined with type II Portland cement and aluminum sulfate accelerator (1.2 Molarity) in varying proportions, denoted as (Acrylic: Cement: Al2SO4 by weight = 5:0.5:0.5, 5:0.75:0.5, 5:1:0.5, and 5:1.5:0.5). The cement content was adjusted while maintaining constant polymer weight and aluminum sulfate proportions. The selection of a 0.5 ratio for aluminum sulfate (1.2 M) was determined by the

consideration that a higher quantity would significantly reduce the cement's fluidity. Table.2 presents the physical and chemical specifications of the liquid polymer.

2.3 Polyurethane (PU)

This study employed hydrophobic foam (Seal Boss 1510) derived from diphenylmethane diisocyanate MDI polyurethane. Its gelling time was regulated by integrating a 15x accelerator. Table. 2 provides the physical and chemical specifications of the polyurethane (PU).

The foam reaction varies depending on the accelerator quantity. Higher percentages of accelerator result in heightened reactivity, shorter hardening time, greater expansion, and reduced density.

Table 2: physical and chemical specifications of the acrylic and polyurethane components.

Property	Acrylic	Seal Boss1510	Accelerator
Appearance	Milky	Amber	Clear
Density	0.99 g/cm^3	1.12	0.93
Viscosity, cps	3	160-250	20
Solubility in water	Dilutable	Not	Not

2.4 Sample Treatment

Fig.3 depicts the schematic composition of both polyurethane and acrylic polymer liquid materials. In the acrylic polymer liquid process, a set quantity of acrylic polymer is initially blended with various cement proportions, designated as (ARC 5:0.5, ARC 5:0.75, ARC 5:1, and ARC 5:1.5). Subsequently, a fixed amount of aluminum sulfate is introduced to the mixture of cement and acrylic polymer. For the polyurethane application, a compound with a 5% accelerator ratio is utilized. The materials are poured in four layers, with a total thickness of 2 mm covering the surface and hole diameter of the samples. A total of five treated samples were employed in this study.

2.5 Dissolution test

The laboratory setup employed in this experiment facilitates the simulation of dissolution tests under low pressures. Fig.4 illustrates the schematic of the dissolution testing apparatus. This device comprises two main components: the water supply and control system, and the test cell. The water supply and control system consist of a pump and pump tank, a variable height upstream tank, a fixed height downstream tank, and a downstream pump. Meanwhile, the test cell comprises an upstream flow chamber, a downstream flow chamber, and a central cell.

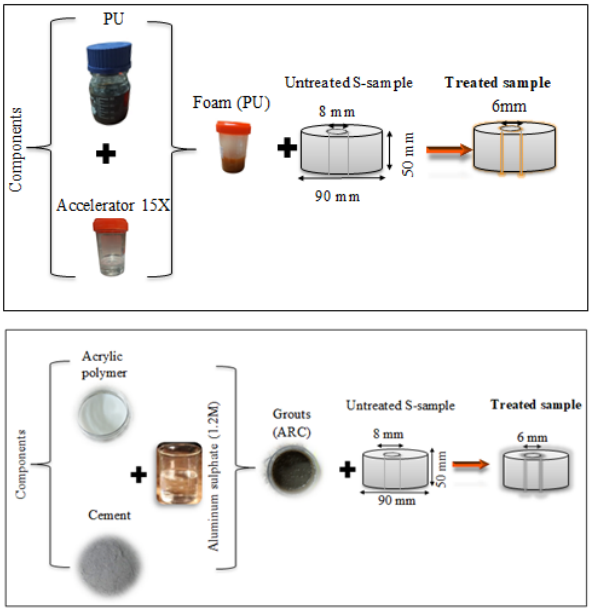

Fig.3: Schematic illustration of the sample treatment procedure, a) ARC and b) PU.

The pump moves 100 liters of water from the pump tank to the upstream tank. Then, water is directed into the test cell by opening the valve of the upstream tank, and any surplus water returns to the pump tank. As water enters the test cell, it flows through the hole's diameter into the downstream tank, gradually expanding the hole's diameter (in case of untreated samples). The water volume in the downstream tank was measured and sent back to the pump tank through the downstream pump for recirculation. Pressure values were monitored using manometers placed in both the upstream and downstream flow chambers.

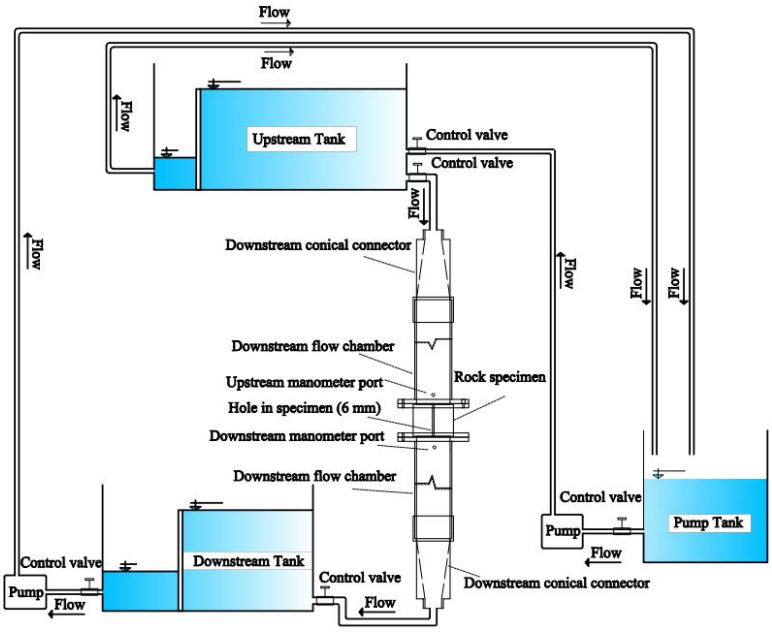

Fig.4: Schematic illustration of the dissolution test apparatus.

3.7 Other tests

Electrical conductivity (EC) of the water samples was measured using ATC (Automatic Temperature Compensation) equipped device.

To measure the dissolved gypsum content in the water samples from the untreated tests, the EDTA titration method proposed by [14] was used. In this procedure, 50 ml of the water sample was measured with a pipette and poured into a clean conical flask. Then, 10 ml of a buffer (1 M NH4OH) solution was added to the flask to reach a pH of 10-11, followed by the addition of a Eriochrome Black T indicator.

The titration began with the gradual addition of the standardized EDTA (0.01 M Ethylenediaminetetraacetic acid) solution from a burette to the sample solution in the conical flask. The titration reached its endpoint as the solution changed color from red to blue, indicating the reaction between EDTA and calcium ions. The recorded EDTA volume was utilized to calculate the quantity of dissolved calcium using Eq.1. To improve result accuracy, the test was iterated three times, and the mean of the finds was taken.

$$Ca^{+2}\ (mg\ /\ lit) = \frac{E \times M \times 40000}{water\ sampel\ (ml)} \quad (1)$$

Where, E is the volume of EDTA and M is the molarity of EDTA (0.01).

4. Results and Discussion

4.1 Untreated Samples

Fig.5 illustrates the results of the solubility test performed on untreated gypsum rock under various constant pressures. In the sample subjected to a constant pressure of ΔH=40 cm, the flow rate increased from 3.3 L/min to 5.9 L/min over a duration of 15,300 seconds, resulting in an average final hole diameter of 9 mm. Under a constant pressure of ΔH=80 cm, the flow rate rose from 7.14 L/min to 15.34 L/min during the same timeframe, with an average final hole diameter of 10.5 mm. Similarly, in the sample exposed to a constant pressure of ΔH=160 cm, the flow rate climbed from 10.24 L/min to 17 L/min, and the average final hole diameter reached 13.5 mm after 15,300 seconds. Table.3 provides the results of the dissolution test of the untreated samples under different pressure. These findings suggest that increasing the pressure upstream of the sample leads to higher flow rates and larger final hole diameters, indicating an enhancement in gypsum rock solubility at low pressures as the pressure increases.

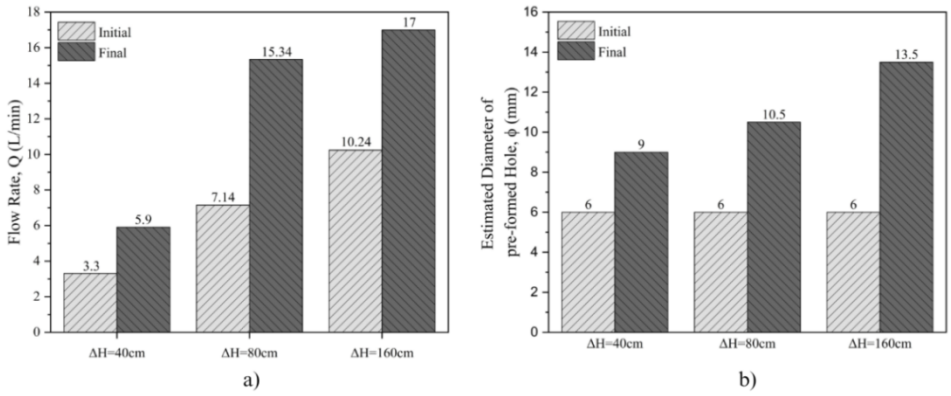

Fig.5: Solubility test results in untreated state; (a) flow rate at initial and final; (b) Hole diameter at initial and final.

Table 3: Solubility test results in untreated state under different pressure.

ΔH (cm)	Q (L/min)		φ(mm)	
	Initial	Final	Initial	Final
40	3.3	5.9	6.0	9.0
80	7.14	15.34	6.0	10.5
160	10.24	10.24	6.0	13.5

In Fig. 6a, the relationship between changes in flow rate over time is depicted. A linear correlation exists between time and flow rate alterations, with regression coefficients of 0.98 at ΔH=160cm, 0.99 at ΔH=80cm, and 0.97 at ΔH=40cm. At all pressure levels, the hole diameter initially increases steeply before gradually declining. Moreover, the trend becomes steeper with higher pressure levels. Fig. 6b illustrates the trend of hole diameter changes over time. There is a linear correlation between time and changes in hole diameter, with regression coefficients of 0.94 at ΔH=160cm, 0.98 at ΔH=80cm, and 0.94 at ΔH=40cm. As pressure increases, the initial flow rate also rises.

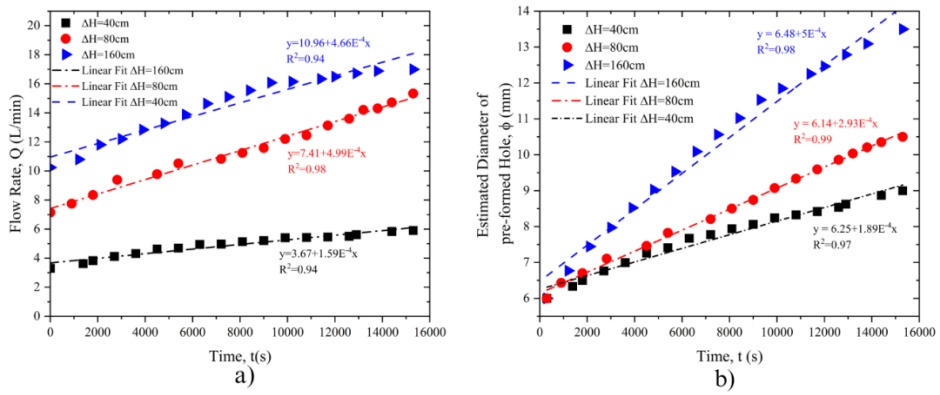

Fig.6: the process of changes in flow rate and hole diameter over time in untreated state; (a) flow rate; (b) Hole diameter.

Fig.7 displays the results of the titration and electrical conductivity tests. The findings indicate a gradual increase in the calcium content in the water over time. Additionally, as the calcium content rises, the water conductivity also increases. In the test when the rock sample subjected to ΔH=160 cm pressure, the calcium concentration in the water sample is notably higher compared to the other samples, indicating higher solubility at this pressure level. Consequently, the hole diameter under this pressure is larger than that under other pressures, consistent with the results of the solubility test. Furthermore, the electrical conductivity results corroborate the increase in solubility with increasing pressure.

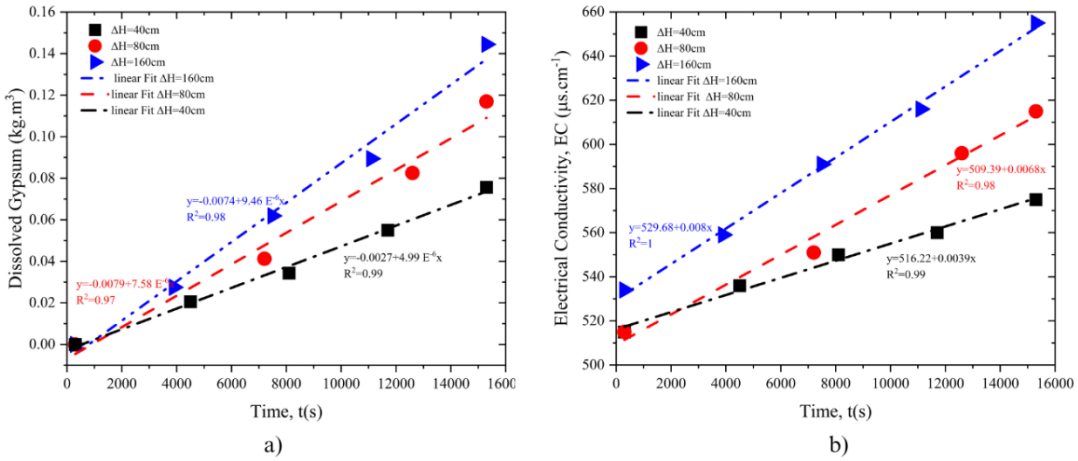

Fig.7: Calcium titration and electrical conductivity test results; (a) amount of gypsum dissolved; (b) Electrical conductivity.

Fig.8 illustrates the correlation between dissolved gypsum and electrical conductivity. It is evident that there exists a linear relationship between the amount of dissolved gypsum and electrical conductivity across all pressures, with regression coefficients close to 1. Specifically, the linear regression coefficient is 1 at ΔH=160cm, 0.98 at ΔH=80cm, and 0.97 at ΔH=40cm. Consequently, electrical conductivity emerges as one of the primary parameters influencing the quantity of gypsum dissolution.

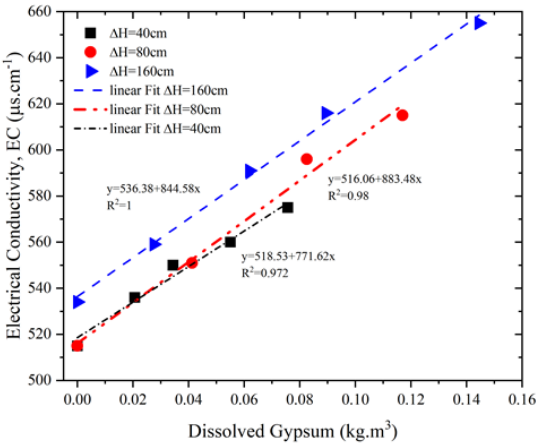

Figure 8: The relationship between dissolved gypsum and electrical conductivity at different pressures.

4.2 Treated Samples

Table.4 provides the dissolution test results of the treated samples. Fig.9 presents the histogram of the results. The findings reveal that when polyurethane and acrylic polymer are utilized with the cement ratios ARC (5:0.5), ARC (5:0.75), the flow rate remains constant at both the beginning and end of the test, resulting in no change in the hole diameter. Conversely, when the ratio of cement to ARC (5:1.5), ARC (5:1) in acrylic polymer is employed, the flow rate increases at the end of the test compared to the beginning, consequently leading to an increase in the hole diameter. Specifically, with the ratio of cement ARC (5:1) in acrylic polymer, the hole diameter increases from 6 mm to 6.2 mm, and the flow rate

Table 4: Solubility test results of the treated samples.

Treated samples	Q (L/min)		φ(mm)	
	Initial	Final	Initial	Final
PU (5.0% acc)	11.3	11.3	6.0	6.0
ARC (5:0.5)	11.3	11.3	6.0	6.0
ARC (5:0.75)	11.3	11.3	6.0	6.0
ARC (5:1.0)	11.31	12.06	6.0	6.2
ARC (5:1.5)	11.29	12.28	6.0	6.5

increases from 11.31 L/min to 12.06 L/min. Similarly, with the ratio of cement ARC (5:1.5) in acrylic polymer, the hole diameter increases from 6 mm to 6.5 mm, and the flow rate increases from 11.29 L/min to 12.28 L/min. Hence, there is a greater likelihood of dissolution occurring when a higher proportion of cement is utilized.

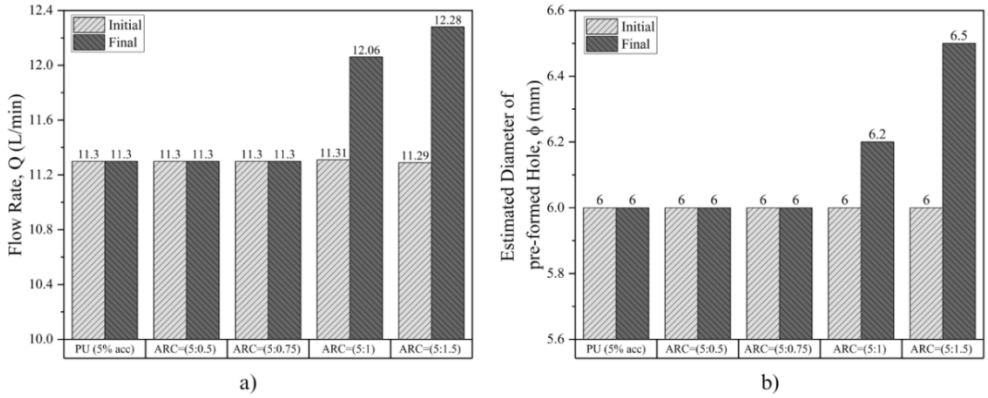

Fig.9: Solubility test results in treatment state; (a) flow rate at initial and final; (b) Hole diameter at initial and final.

Fig.10 displays the results of changes in flow rate and hole diameter over time in the treated state. The results suggest that when polyurethane and acrylic polymer are utilized with the cement ratios ARC (5:0.5) and ARC (5:0.75), the flow rate remains consistent throughout the test, leading to no alteration in the hole diameter. However, when the ratio of cement in the mixture of ARC reached (5:1.5) and (5:1), both the flow rate and hole diameter exhibit linear increases. Specifically, in the case of the cement ratio ARC (5:1) in acrylic polymer, the regression coefficient is 1 for flow rate and 0.98 for hole diameter, respectively. Similarly, for the cement ratio ARC (5:1.5) in acrylic polymer, the regression coefficients are 0.98 and 0.84 for flow rate and hole diameter, respectively.

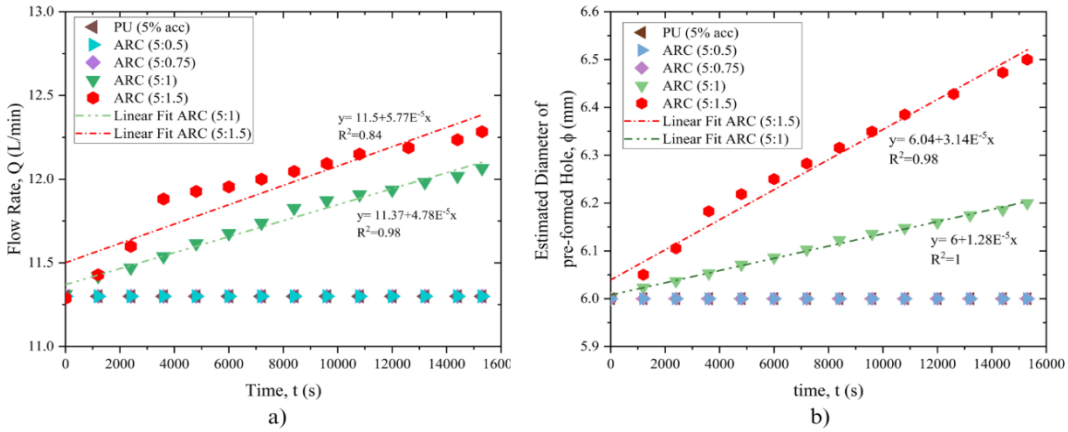

Fig.10 the process of changes in flow rate and hole diameter over time in treatment state; (a) flow rate; (b) Hole diameter.

5. Conclusion

The aim of this study is to examine the solubility of gypsum rock and methods for treating its solubility. The findings of this investigation can be summarized as follows:

- Solubility of gypsum rock occurs even under low pressures, and its solubility increases as pressure rises.
- The consistent hole diameter maintained when employing the polyurethane treatment method indicates robust adhesion of this material to gypsum rock and its hydrophobic properties.
- The acrylic polymer treatment method shows that the hole diameter varies with increasing cement ratio. Therefore, the optimal ratio for this method can be considered as the limit ARC (5:1), effectively preventing dissolution in gypsum rock.

References

[1] N. Adamo, N. Al-Ansari, I. Issa, V. Sissakian, and S. Knutsson, "Mystery of Mosul dam the most dangerous dam in the world: Foundation treatment during construction," *Journal of Earth Sciences and Geotechnical Engineering,* vol. 5, no. 3, pp. 59-69, 2015.

[2] N. Adamo, N. Al-Ansari, J. Laue, S. Knutsson, and V. Sissakian, "Risk management concepts in dam safety evaluation: Mosul Dam as a case study," *Journal of Civil engineering and architecture,* vol. 11, no. 7, pp. 635-652, 2017.

[3] K. D. Weaver and D. A. Bruce, *Dam foundation grouting*. ASCE press Reston, VA, 2007.

[4] L. Li, S. Li, Q. Zhang, J. Cui, Z. Xu, and Z. Li, "Experimental study of a new polymer grouting material," *Chin. J. Rock Mech. Eng,* vol. 29, pp. 3150-3156, 2010.

[5] P. K. Kolay, B. Dhakal, S. Kumar, and V. K. Puri, "Effect of liquid acrylic polymer on geotechnical properties of fine-grained soils," *International Journal of Geosynthetics and Ground Engineering,* vol. 2, pp. 1-9, 2016.

[6] C. Vipulanandan, M. B. Kazez, and S. Henning, "Pressure-temperature-volume change relationship for a hydrophilic polyurethane grout," in *Grouting and deep mixing 2012*, 2012, pp. 1808-1818.

[7] L. R. León and C. Matthews, "Storm water quality handbooks: construction site best management practices (BMPs) manual," 2003.

[8] F. Khelifa, Y. Habibi, and P. Dubois, "Nanocellulose-based polymeric blends for coating applications," in *Multifunctional polymeric nanocomposites based on cellulosic reinforcements*: Elsevier, 2016, pp. 131-175.

[9] K.-T. Chhun, S.-H. Lee, S.-A. Keo, and C.-Y. Yune, "Effect of acrylate-cement grout on the unconfined compressive strength of silty sand," *KSCE Journal of Civil Engineering,* vol. 23, pp. 2495-2502, 2019.

[10] M. Y. Fattah, M. M. Al-Ani, and M. T. Al-Lamy, "Studying collapse potential of gypseous soil treated by grouting," *Soils and Foundations,* vol. 54, no. 3, pp. 396-404, 2014.

[11] M. K. Faris, "Evaluating the Stabilization of Gypseous and Gypsiferous Sands Using Different Chemical Additives to Mitigate Gypsum Dissolution," University of South Carolina, 2020.

[12] A. Nikolaev and E. Foregina, "Protective effect of films on gypsum," *Protective Films on Salts,* 1944.

[13] W. Buggakupta, K. Tounchuen, W. Panpa, and S. Jinawath, "Early production of high strength and improved water resistance gypsum mortars from used plaster mould and cullet waste," *Journal of Materials in Civil Engineering,* vol. 32, no. 6, p. 04020116, 2020.

[14] G. Horvai, "Gary D. Christian, Purnendu (Sandy) Dasgupta and Kevin Schug: Analytical chemistry," ed: Springer, 2014.